Hindawi
Geofluids
Volume 2023, Article ID 4791411, 12 pages
https://doi.org/10.1155/2023/4791411

Research Article

Layout and Parameter Analysis of the Cooling System with Mine Water as Cold Source in Linglong Gold Mine

Chunlong Wang,[1] **Hongkai Zhao**,[2] **Li Cheng**,[1] **Guilin Li**,[1] **Yuyun Fan**,[1] **Mingwei Jiang**,[1] **Yingjie Hao**,[1] **and Kun Shao**[3]

[1]*Deep Mining Laboratory of Shandong Gold Group Co., Ltd., Yantai, China*
[2]*Sanshandao Gold Mine, Shandong Gold Mining (Laizhou) Co., Ltd., Yantai, China*
[3]*Shandong Institute of Advanced Technology, Jinan, China*

Correspondence should be addressed to Chunlong Wang; 416773656@qq.com

Received 18 April 2023; Revised 14 July 2023; Accepted 19 July 2023; Published 29 July 2023

Academic Editor: Constantinos Loupasakis

Copyright © 2023 Chunlong Wang et al. This is an open access article distributed under the Creative Commons Attribution License, which permits unrestricted use, distribution, and reproduction in any medium, provided the original work is properly cited.

As the heat hazard problem in the deep mine becomes more prominent, it is difficult to alleviate the high-temperature problem by increasing the air supply and adjusting the ventilation mode alone. In order to solve the issue of heat damage in the Linglong Gold Mine, a cooling system based on water source heat pump technology and utilizing the return air system to exhaust heat was constructed, and each system was rationally arranged in conjunction with the mine's actual conditions. The reasonable critical threshold of cooling system parameters is then determined by numerical simulation and field application verification. The results indicate that the closed cycle adopted by the cooling system can effectively solve the problem of groundwater shortage. The heat can be discharged directly to the return air shaft to prevent the impact of secondary heat hazards. The temperature near the working face can be reduced from 35°C to below 28°C. This system effectively resolves the issues of water shortage, heat release, and cold transfer in the water source heat pump technology and provides a reference for the application of other mines.

1. Introduction

With the continuous deepening of the mine and the continuous improvement of the mine's mechanization level, the heat sources, such as the exothermic heat of the deep surrounding rock and the heat of the air compression, are significantly increased. As a result, the heat hazard problem of the single long-distance heading and the stope is becoming more and more severe. During shallow production, ventilation is frequently used to improve the stope's thermal environment. However, the air intake and geothermal temperature in the deep levels are higher than in the shallow levels. Therefore, the cooling effect gradually decreased as the ventilation and cooling technology's cooling capacity and ventilation limit decreased. Increasing the air supply and adjusting the ventilation mode is insufficient to alleviate the problem of high temperatures. Therefore, artificial cooling is typically used to improve the underground thermal environment during deep well mining [1].

Since the 1970s, artificial cooling technologies such as air conditioning, ice cooling, and water cooling have developed rapidly [2–4]. However, technology for cooling air conditioners has advanced earlier. A surface- or underground-mounted centralized cooling system is typically used to address the issue of heat hazards. This system entails installing a refrigerating unit on the ground or underground, transporting chilled water to the cooler via a pipeline, and sending cold air to the worker's face via an air cooler. This technology has a complex system, is difficult to install and maintain, and is expensive to operate. Many mines have adopted ice cooling technology [5, 6]. Ice's initial temperature is lower than water's, and its transportation speed is faster. However, as mine depth and cooling load increase, the cost of pumping chilled water increases significantly, and cooling loss along the way is greater.

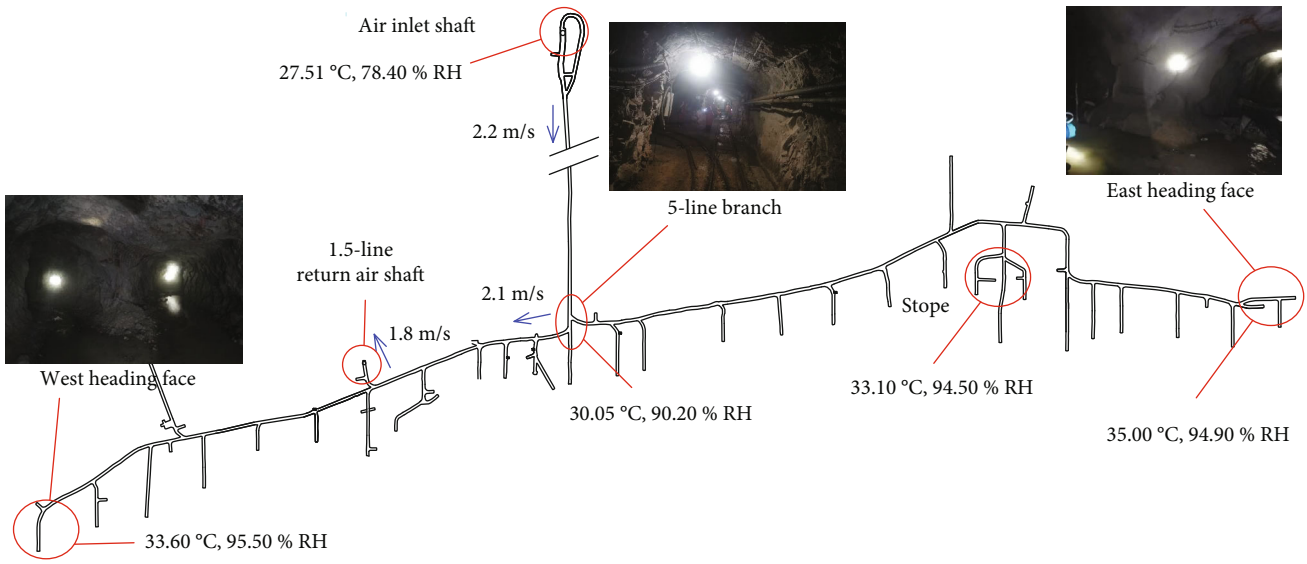

Figure 1: Measured results of the thermal environment at -750 m level.

Based on those two technical issues, numerous researchers have proposed the water source heat pump cooling technology with underground water as the cold source [7–17], which uses the water source heat pump unit to extract the heat from the mine water and alleviate the high-temperature and high-humidity operating environment in the mine. It has been successfully applied to various types of coal mines and noncoal mines [18–22]. Professor He Manchao proposed a HEMS cooling system that uses mine water as a cold source based on water source heat pump technology. Its working principle is to use mine water to extract cold energy from mine water through an energy extraction system and exchange heat with high-temperature air in the working face to improve the working environment. At the same time, the replaced heat is discharged to the surface using water as a carrier [23, 24]. This method utilizes mine water as a cold source with low energy consumption, low initial investment, and low operating costs; it can also recover the residual heat in mine groundwater; however, its cooling efficiency is low, and it has stringent requirements for mine groundwater. The heat hazard control effect of this technology has been significant in coal mines and noncoal mines [25–29]. Due to the varying operating conditions of each mine, the layout structure, operation parameters, construction cost, and operating cost of the water source heat pump cooling system are very different and must be designed accordingly. According to the actual situation of each mine and the distribution law of tunnel temperature field, many scholars have analyzed and optimized water source heat pump cooling technology in terms of heat hazard control mode, temperature control technology evaluation system, water source composition, design basis, refrigeration parameter calculation, and cold source shortage compensation [30–35]. In addition, some scholars [36–39] have designed injection and production channels below the ventilation tunnel, which can effectively improve the thermal environment of the tunnel by cooling the surrounding rock of the tunnel with low-temperature water and exploiting mine geothermal energy.

Due to the incompletely established ventilation system in the Lingshan area, the problem of heat hazard caused by this is prominent, and the thermal environment of the operation site cannot be improved by increasing air intake. Using the -750 m level as the research object, the cooling range consists of two heading working faces and two stope working faces. Combining underground production and existing conditions, this paper proposes a cooling systems based on water source heat pump technology and using the underground return air system to exhaust heat. The thermal environment distribution law of the transportation tunnel is simulated and analyzed by constructing the deep middle section's heat and mass transfer model. The optimal inlet air temperature and speed threshold are determined. It serves as a guide for selecting and installing the technical parameters of the cooling system.

2. Mine Background

Lingshan area of Linglong Gold Mine of Shandong Gold Group is in Zhaoyuan City, Shandong Province. The current depth of mining is -870 m. The mine uses a vertical shaft and a blind inclined shaft in combination for development. The principal mining techniques are downward horizontal slicing and downward drift mining. Mechanical extraction ventilation and a diagonal ventilation system are used in the mining area. Fresh air enters the subterranean environment through the tunnel via the shaft and inclined shaft and enters the working faces. The dirty air travels through the upper and middle return air tunnels, the inverted air shaft, and the 2-line return air shaft before being discharged to the surface after washing the working faces. A 5-line shaft supplies the -750 m level of fresh air, and the 1.5-line air return shaft is used for air return. The mining operation site is a two-wing heading face with two stopes. The four mining working faces can only be cooled by local ventilation because the ventilation system is still in its infancy and is far from the air return system. According to the results of the field tests depicted in Figure 1, the temperature and humidity of the

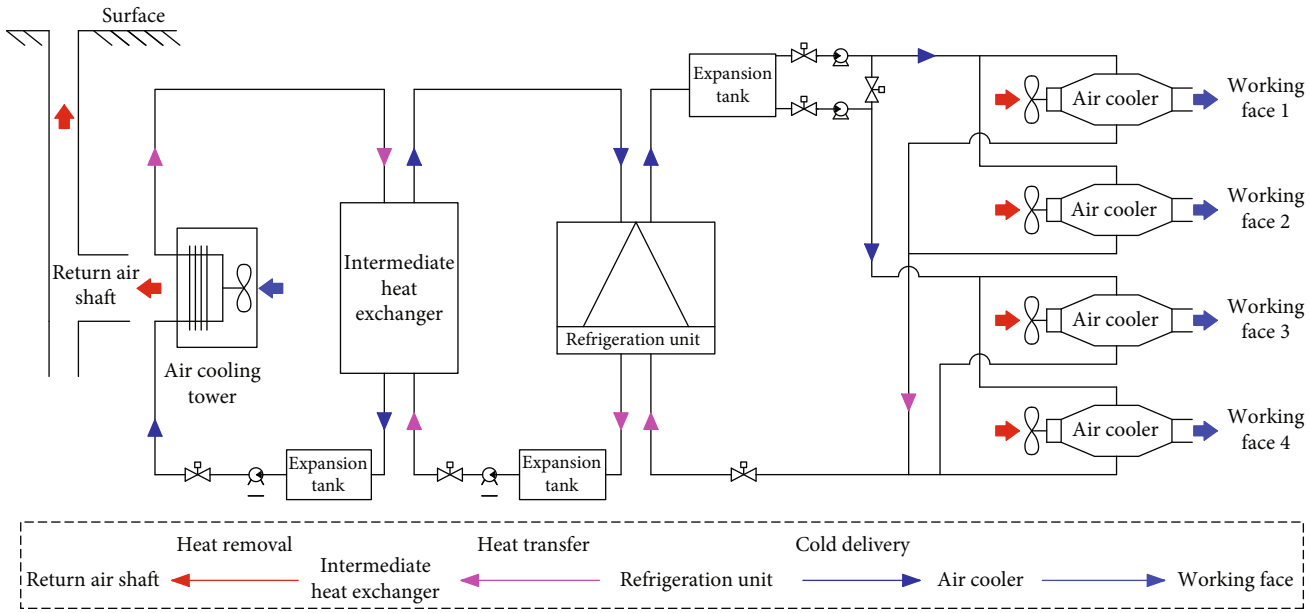

Figure 2: System composition.

working faces at the -750 m level are relatively high, especially given the distance between the east heading face and the return air shaft of line 10 (about 700 m). The wall temperature is approximately 38°C, and the operating environment temperature can reach 35°C due to the heat released by surrounding rock and mechanical equipment. Therefore, ventilation cannot be used to increase the temperature of the working environment.

3. Cooling System Layout

3.1. System Composition. In the past, the water source heat pump technology utilized a large amount of underground low-temperature water inrush to replace the heat of the working face with a large amount of hot water and discharge it to the level water sump. This method necessitates a significant amount of low-temperature water inrush, significantly increasing drainage costs. In addition, the hot water discharged in the tunnel and water sump will create a secondary heat hazard that is not conducive to ventilation and cooling. According to the field investigation and test, the chloride ion content of the fissure water at -630 m level is 134 mg/L, the water quality is good, and the water temperature is appropriate (27°C). However, the amount of water used is small. Therefore, a cooling system based on water source heat pump technology and employing underground return air systems to exhaust heat is proposed in conjunction with the underground geological conditions, ventilation mode, and topological structure of the Lingshan area. The refrigeration, cold delivery, heat transfer, and heat removal systems are the four components that make up the cooling system, as shown in Figure 2. A fully closed cycle serves as the working medium.

(1) Cold delivery system: the hot and moist air exchanges heat with the chilled water in the pipeline through the air cooler and is sent to the working face after the temperature drops. After the chilled water absorbs heat, the temperature rises and is transported to the refrigeration unit through a return water circulation pump. The refrigeration unit cools the chilled water and then sends it back to the air cooler in the mining area to complete the cycle. Multiple working faces' air coolers are connected in parallel

(2) Heat transfer system: the refrigeration unit transfers heat to the condenser end via the steam compression refrigeration cycle, and the cooling working medium, which is driven by the circulating pump of the intermediate circuit, transfers heat to the hot end of the intermediate heat exchanger. After the intermediate heat exchanger completes the heat exchange, the heat is transferred to the cold end of the intermediate heat exchanger. The cooling medium, driven by the circulating pump of the cooling circuit, is then transferred to the return air cooling tower

(3) Heat removal system: the return air cooling tower uses the wind in the return air system as the cold source and finally removes the heat from the ground to the ground

3.2. System Layout. Following the operating principle, the air cooler is positioned close to the stopes and heading faces. The refrigeration unit and the intermediate heat exchanger are positioned at the 5-line of the intake airway, and the distance between them and the working faces on both sides is appropriate, which can reduce the cold loss along the way and is conducive to the heat dissipation and management of the unit. The air cooling tower is positioned at the 1.5-line working air shaft to discharge heat directly to the return air shaft. The system's circulating water is supplied by a low-

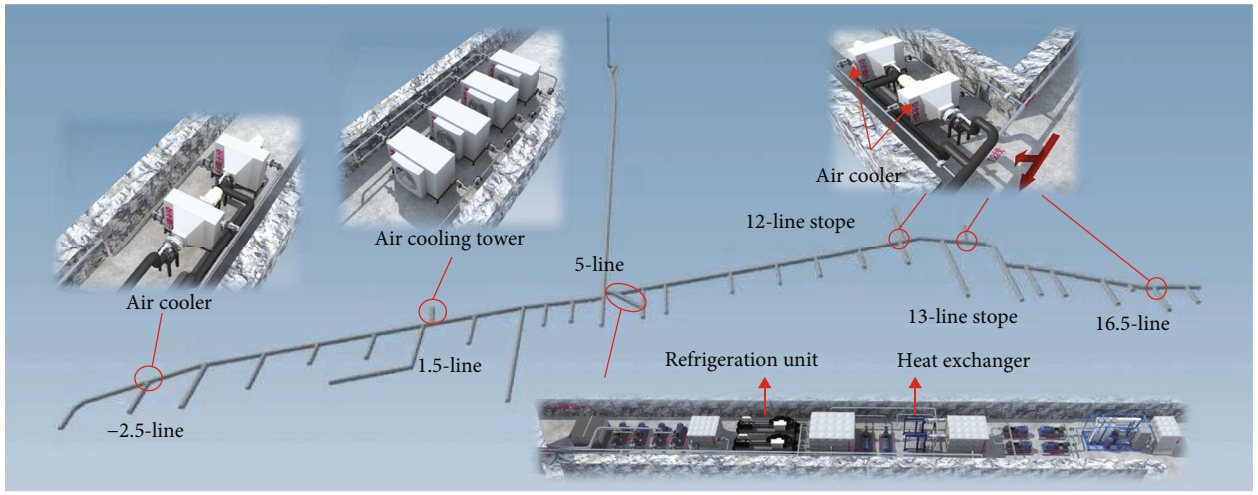

Figure 3: System layout.

Table 1: Load calculation results.

	Mechanical equipment power (kW)	Heat load of mechanical equipment (kW)	Sensible heat load of surrounding rock and ponding (kW)	Latent heat load of surrounding rock and ponding (kW)	Total heat load (kW)
Stope ① and heading face ①	30.00	12.05	11.74	28.14	51.93
Stope ② and heading face ②	45.00	18.05	11.74	28.14	57.93
Total					219.72

temperature water inflow at a level of -630 m that, after filtration, flows into the closed circulation. Figure 3 depicts the precise equipment configuration.

The system gradually transfers heat from the stope to the return air flow via the air cooler installed in the working face, the refrigeration unit and intermediate heat exchanger installed in the tunnel, and the air cooling tower installed in the return air shaft. As a result, low energy consumption and low initial cost are characteristics of this system. In addition, due to the shortage of underground water sources, a closed cycle system is adopted, which has lower requirements for water quality and quantity, and equipment operation is more stable and reliable. The traditional heat removal process is to directly discharge heat into the tunnel or water sump, causing the temperature of the tunnel to rise. However, this system directly discharges heat into the return air shaft, thereby avoiding the secondary impact of the heat removal process on the tunnel's air environment.

4. Load Calculation

4.1. Working Face Load Calculation. According to the on-site investigation results, the specific parameter settings are as follows:

(1) Surrounding rock and ponding: according to the field measurement data, the surrounding rock temperature is about 38°C. There is usually a layer of ponding at the bottom of the tunnel due to poor drainage. According to the field survey results, the average width of the ponding set in the tunnel is 2 m, and the temperature is 2°C lower than the wall temperature

(2) Design parameters of tunnel air conditioning: the design target parameters are taken as 28°C and relative humidity 85% RH, and ventilation wind speed in the mining area is 0.5 m/s

(3) Equipment and personnel: based on the survey results, the following assumptions are made: there are two stopes and two heading faces working at the same time in -750 m level, the number of workers in stope ① and heading face ① is two, the equipment is two rock drilling jumbos, and the power consumption is 30 kW; the number of workers in stope ② and heading face ② is two, and the equipment is a forklift, with a power consumption of 45 kW. The utilization factor of the two equipment is set to 0.5

Set the design temperature of the working face to 28°C, and the outdoor point air parameters are 35°C and 70% RH. The load calculation results are shown in Table 1.

4.2. Cooling Load Calculation. The load of the air cooler decreases first and then increases within a reasonable range as the inlet air temperature rises. Therefore, to ensure the

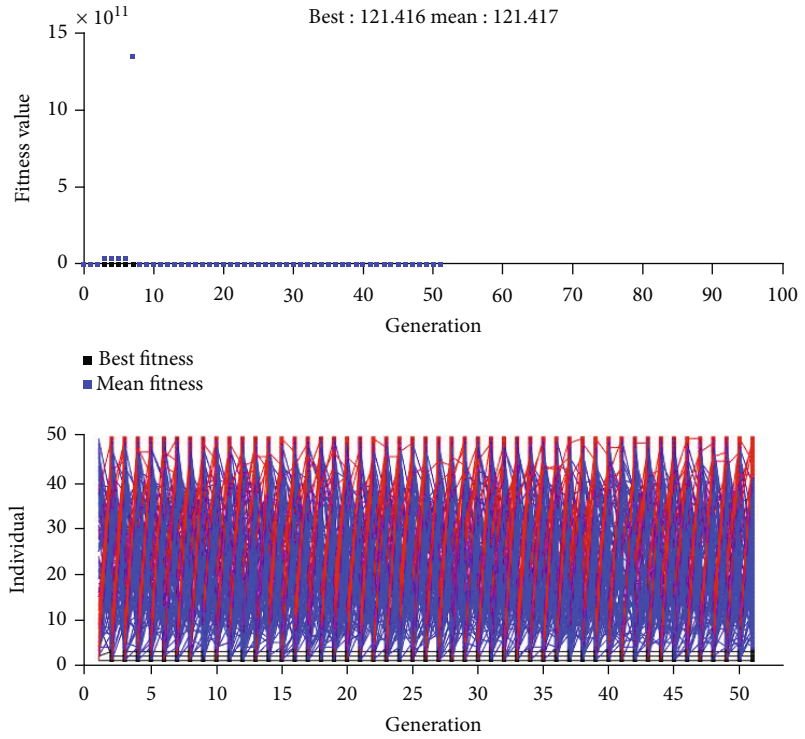

Figure 4: Calculation process of the genetic algorithm.

Table 2: Cooling load calculation results.

	Inlet air volume (m/s)	Mechanical equipment power (kW)	Heat load of mechanical equipment (kW)	Sensible heat load of surrounding rock and ponding (kW)	Latent heat load of surrounding rock and ponding (kW)	Total heat load (kW)	Cooling load (kW)
Stope ① and heading face ①	1.03	30.00	12.05	11.74	28.14	51.93	76.80
Stope ② and heading face ②	1.14	45.00	18.05	11.74	28.14	57.93	85.68
Total						219.72	325.00

ventilation effect, it is necessary to optimize the inlet air parameters of the air cooler to reduce its load.

Set the tunnel air temperature to 35°C with a relative humidity of 70% RH and a gas pressure of 0.12 MPa; take 28°C as the design temperature of the working face; take 35°C and 70% RH as the outdoor point air parameters; and use the genetic algorithm to calculate the optimal inlet air parameters under the minimum cooling load, as shown in Figure 4.

Under a reasonable range of inlet air parameters, the optimization results show that the lower the inlet air temperature, the smaller the inlet air volume and the smaller the system's cooling load. Using 14°C as the set inlet air temperature, MATLAB is utilized to calculate the inlet air volume and cooling capacity that meets the design requirements. The results are shown in Table 2. According to the results, the total cooling load of the two stopes and two heading faces at -750 m level is approximately 325 kW, and the redundancy coefficient is 1.3. The total cooling load is 420 kW, and a load of a single air cooler is 105 kW. This result can be used as the primary criterion for system design and equipment selection.

5. Optimization of Inlet Air Parameters

Typically, there are two ways to reduce the air temperature in a space: increasing the ventilation speed or decreasing the ventilation temperature. However, both of these methods will increase the cooling pressure in the system. Therefore, to improve the economics of the cooling ventilation system, it is crucial to select appropriate ventilation parameters and reduce cooling energy consumption as much as possible under the premise of achieving the target temperature.

5.1. Theoretical Calculation. Since the east heading face of the -750 m level is the farthest from the intake airway and has the highest temperature and humidity, the heading face is taken as the reference point to calculate the inlet air

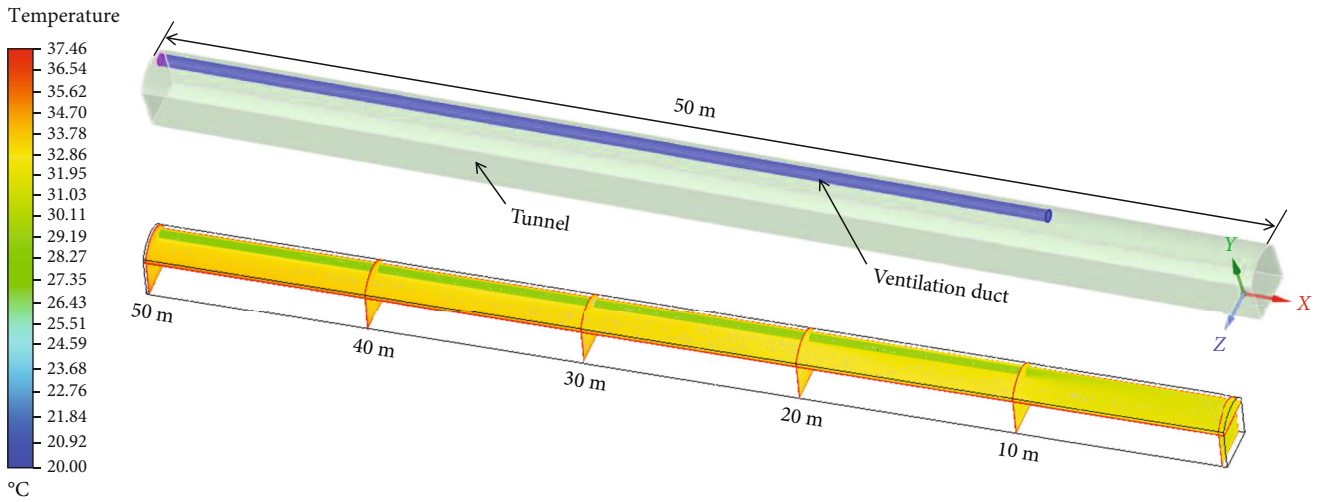

Figure 5: Heading face model and temperature field distribution law.

Table 3: Comparison of temperature simulation results.

Distance from working face (m)	Measured temperature (°C)	Simulated temperature (°C)	Temperature difference (°C)
1	32.9	34.0	1.1
10	33.5	34.3	0.7
20	34.2	34.8	0.6
30	34.5	35.0	0.5
40	34.7	35.2	0.5
50	34.8	35.2	0.4
Average temperature	34.1	34.8	0.7

temperature. Other parameters can be calculated using the heat load back analysis method [31]. According to the heating rate and the target temperature of the working face T_C', the inlet air temperature T_A' can be finally obtained:

$$\begin{aligned} T_A' &= T_C' - \beta_2 \Delta T_{BC} \cdot \frac{L_{BC}}{100} - \beta_1 \Delta T_{AB} \cdot \frac{L_{AB}}{1000}, \\ \Delta T_{AB} &= \frac{T_B - T_A}{L_{AB}} \cdot 1000, \\ \Delta T_{BC} &= \frac{T_C - T_B}{L_{BC}} \cdot 100, \end{aligned} \tag{1}$$

where T_A' is the inlet air temperature (°C), T_C' is the lower corner temperature of working face after cooling (°C), T_A is the inlet air temperature before cooling (30°C), T_B is the corner temperature of working face before cooling (35°C), T_C is the lower corner temperature of working face before cooling (°C), L_{AB} is the control point AB distance (m), L_{BC} is the control point BC distance (m), $\triangle T_{AB}$ is the temperature rise rate of air flow in inlet air tunnel (°C/km), $\triangle T_{BC}$ is the air flow temperature rise rate of working face (°C/km), and β_1 and β_2 are the correction coefficients of temperature rise rate.

The target temperature is 26~28°C. Due to the fact that this area is an excavation tunnel, the temperature rise rate is relatively small, and the correction coefficient for temperature rise rate is greater than that of the return air roadway, so 2-3 is taken. According to the calculation, the intake temperature range is 7.0-14.0°C.

5.2. Model Establishment and Verification. A heat and mass transfer model was established using the fluid simulation software Fluent within a range of 50 m east of the -750 m horizontal plane in the excavation face, as shown in Figure 5. The following are the model's underlying assumptions: only the forced ventilation cooling mode is adopted because it is consistent with the actual site conditions. Transportation roadway specification 2.4 m* 2.6 m. The RNG k-ε model and SIMPLEC algorithm were selected. According to field measurements, the diameter of the ventilation duct in the heading face is 0.5 m, the inlet air speed is 3 m/s, the inlet air temperature is 30°C, the wall temperature is 38°C, and the operating environment temperature is 35°C.

Figure 5 depicts the simulation results for the distribution law of the tunnel temperature field. The cross-section at the height of 1.8 m above the ground and the tunnel profile at a distance of 10 m from the working face is measured, and the average temperature of these measuring points is determined. Table 3 displays the findings. According to

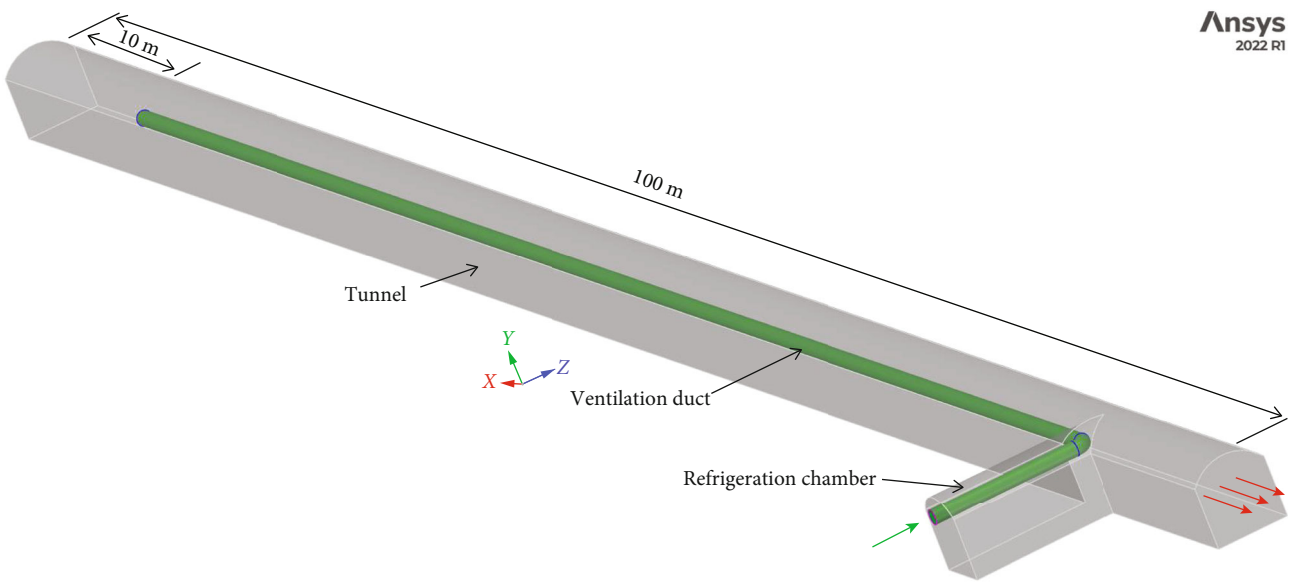

Figure 6: Tunnel geometric model.

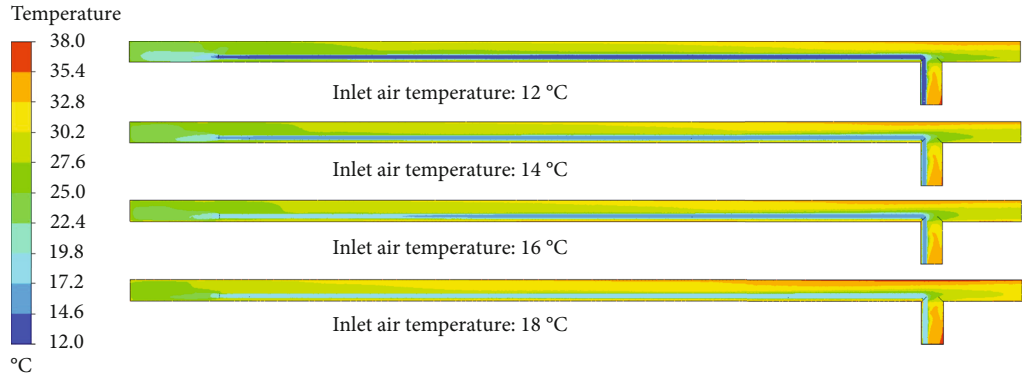

Figure 7: Temperature field distribution of tunnel under inlet air speed of 3 m/s.

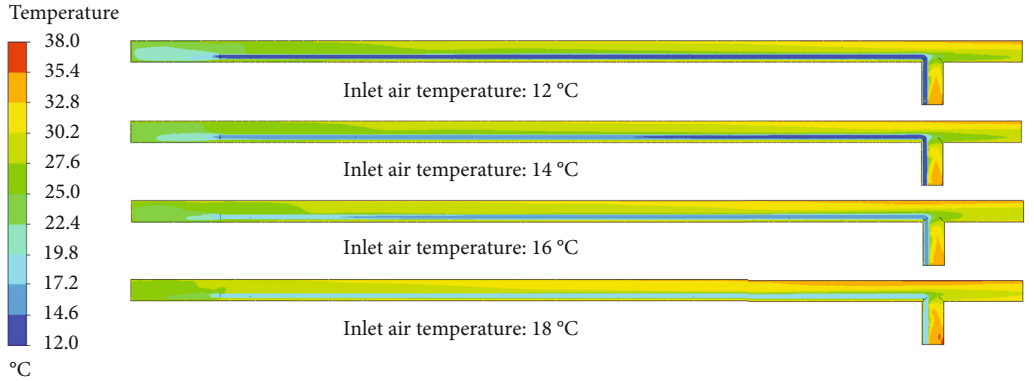

Figure 8: Temperature field distribution of tunnel under inlet air speed of 4 m/s.

the simulation results, the maximum temperature difference between the simulation and test results is at the working face, with a difference of 1.1°C. The temperature difference between 20 m and 50 m is maintained at 0.5°C. The primary cause is the influence of other heat sources, such as mechanical equipment and personnel, on the working face, resulting in a significant

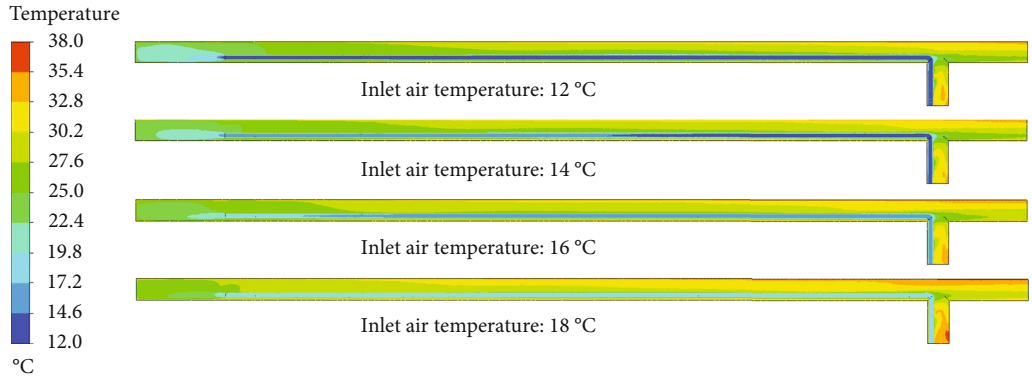

Figure 9: Temperature field distribution of tunnel under inlet air speed of 5 m/s.

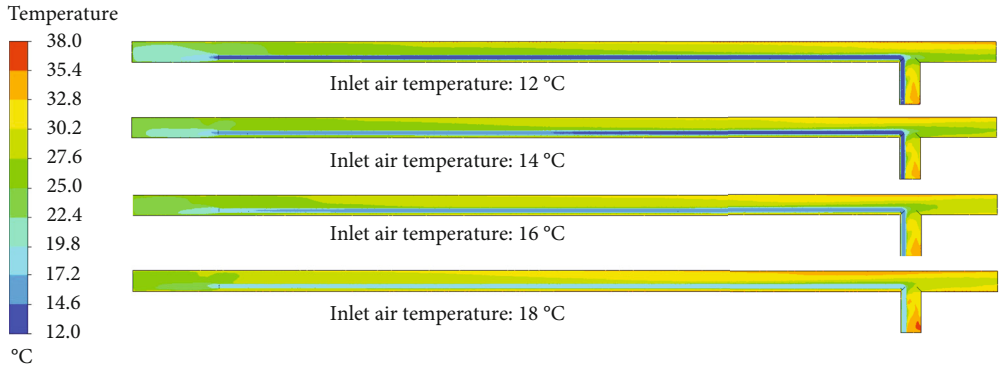

Figure 10: Temperature field distribution of tunnel under inlet air speed of 6 m/s.

temperature difference. The average temperature error within 50 m of the working face is 2%, which is a slight error; therefore, the model agrees with the actual situation.

5.3. Analog Computation. Based on the above model, the tunnel's heat and mass transfer model under refrigeration and ventilation conditions is constructed, and the range of the best inlet parameters is analyzed. The numerical model is shown in Figure 6. First, the refrigeration unit is placed in a chamber approximately 100 m behind the working face to avoid the impact of the blasting shock wave on the refrigeration equipment of the working face. The chamber is equipped with fans and air cooler. Fresh air is sent to the chamber by relay fans, and the fresh air temperature is reduced by air cooler. Then, the cold air is sent to the working face through a ventilation duct with a diameter of 0.5 m, and the ventilation duct is 10 m behind the working face. Due to the pressure difference, dirty air naturally flows back. The surrounding rock is set to 35.0°C.

The inlet speed is set at 3 m/s, 4 m/s, 5 m/s, and 6 m/s. In addition, the inlet temperature is set at 12°C, 14°C, 16°C, and 18°C, respectively, in order to study the impact of wind speed and temperature on the ventilation and cooling effect of the tunnel. By analyzing the distribution law of the tunnel temperature field within 100 m of the working face under 16 different wind conditions, the optimal inlet condition range is determined to achieve the cooling and cost savings goals. In Figures 7–10, the distribution pattern of temperature field under different inlet conditions is depicted.

5.4. Analysis of Temperature Field Distribution. Monitoring points are set at 10 m, 20 m, 30 m, 50 m, 70 m, and 100 m away from the working face, and the results are shown in Figure 11 based on the simulation calculation of the thermal environment of the tunnel under various different inlet speeds and temperatures. The upper limit temperature of the low-temperature area in the figure is 28°C.

Figure 11(a) shows that when the inlet speed is 3 m/s and the inlet temperature is 12°C, the range of low-temperature zone is 38 m within the working face. As a result, the minimum temperature of the working face reaches 25.67°C. When the inlet temperature is between 14°C and 16°C, the temperature difference is minimal, and the temperature within 20 m of the working face can drop below 28°C; when the inlet temperature is 18°C, the tunnel air temperature is above 28°C.

As shown in Figure 11(b), when the inlet speed is 4 m/s and the inlet temperature is 12°C, the low-temperature area is 40 m within the working face, and the minimum temperature of the working face reaches 25.42°C. When the inlet temperature is 14°C, the inlet temperature can drop below 28°C within 30 m of the working face. When the inlet air temperature is 16°C, the inlet temperature is below 28°C within 20 m of the working face; when the inlet

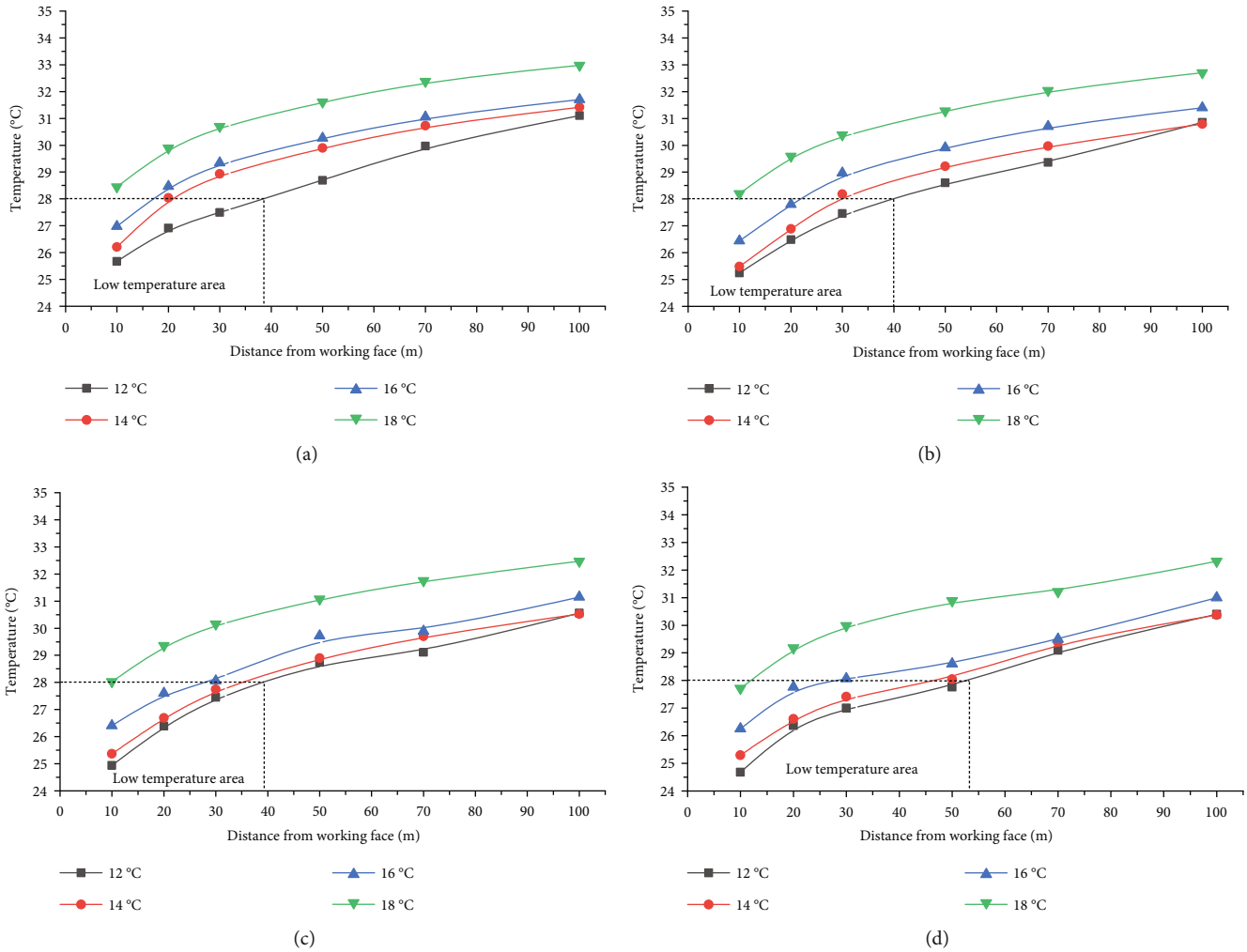

Figure 11: Temperature of each monitoring point under various inlet air temperatures and speeds. (a) The speed is 3 m/s. (b) The speed is 4 m/s. (c) The speed is 5 m/s. (d) The speed is 6 m/s.

temperature is 18°C, the tunnel air temperature is all higher than 28°C.

As shown in Figure 11(c), when inlet speed is 5 m/s and the wind temperature is 12°C or 14°C, the temperature difference at each measuring point is small, and the temperature within about 40 m of the working face drops to below 28°C, and the minimum temperature of the working face reaches 24.94°C. When the inlet temperature is 16°C, the temperature within about 30 m of the working face drops to below 28°C. When the inlet temperature is 18°C, the temperature reaches 28°C within 10 m of the working face.

As shown in Figure 11(d), when inlet speed increases to 6 m/s and the inlet temperature is 12°C or 14°C, the range of the low-temperature area rapidly increases to 53 m, and the temperature difference of each measuring point is small under these two conditions, and the minimum temperature of the working face reaches 24.68°C. When the inlet temperature is 16°C, the temperature can reach below 28°C within 30 m of the working face, and the range changes slightly compared with the wind speed of 5 m/s. When the inlet speed is 18°C, only the temperature within 10 m of the working face can be lower than 28°C.

The analysis of simulation data reveals the following: (1) When the inlet temperature is 18°C, the impact of an increase in inlet air speed on the tunnel temperature field is minimal and exceeds 28°C, which does not meet the temperature requirements. (2) When the inlet temperature is between 12°C and 16°C, the impact of inlet speed on the working face within 10 m is minimal, as indicated by the fact that the minimum temperature change value of the working face is only 0.99°C with an increase in inlet speed. (3) The inlet speed is between 3 m/s and 5 m/s. When the inlet temperature is between 12°C and 14°C, the temperature difference between each measuring point gradually decreases as the inlet speed increases. The range of air temperature below 28°C is stable at about 40 m from the working face, and the range is expanded to about 53 m when the inlet speed is 6 m/s. (4) When the inlet speed is 6 m/s and the inlet temperature is reduced from 14°C to 12°C, the temperature difference at each monitoring point is small, which indicates that the reduction in inlet air temperature has little impact on the tunnel air temperature under this condition.

Figure 12 shows the average temperature distribution within 50 m of the tunnel at different inlet speeds and

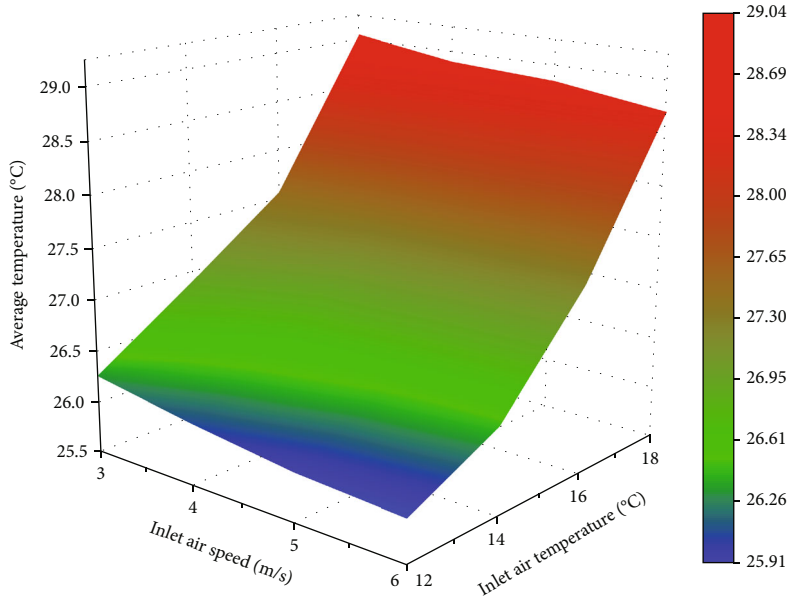

Figure 12: Average temperature distribution in tunnel under varying inlet air speeds and temperatures.

temperatures. According to the findings, when the inlet air temperature is 18°C, the average air temperature in the tunnel at different inlet air speeds is above 28°C. With an inlet speed of 3 m/s to 4 m/s and an inlet temperature of 14°C to 16°C, the tunnel's average air temperature can reach a range of 26°C to 28°C. In the range of 4 m/s to 6 m/s and an inlet temperature of 12°C to 14°C, the cooling effect is optimal, and the average air temperature of the tunnel can reach below 26°C; however, when the air is reduced, the average temperature decreases less, and the impact is minimal.

In conclusion, the thermal environment of the stope can be effectively improved by lowering the inlet temperature or increasing the inlet speed, with lowering the inlet temperature having a more pronounced effect on the thermal environment. The average temperature of the tunnel within 50 m of the working face can meet the specified requirements within the range of inlet speed of 4 m/s to 6 m/s and temperature of 12°C to 16°C. After the inlet temperature is reduced to 14°C, the tunnel air temperature field changes slightly with the inlet speed increasing to more than 5 m/s. Therefore, if the inlet speed is 5~6 m/s and the inlet temperature is 14°C, the tunnel air temperature within 50 m of the working face can drop below 28°C, which can be used as the critical threshold of the inlet parameters.

5.5. Application Analysis. The simulation results are applied to the cooling system of the east heading face, and the equipment installation diagram is shown in Figure 13. The equipment is installed in the chamber about 100 m away from the working face, mainly including air cooler, water inlet pipe, water drain pipe, fan, and ventilation duct. After passing through the air cooler, the temperature of tunnel air is reduced to the design temperature and delivered to the working face, thus improving the thermal environment of the working face. According to on-site testing, the air temperature around the air cooler is about 35.1°C, the water

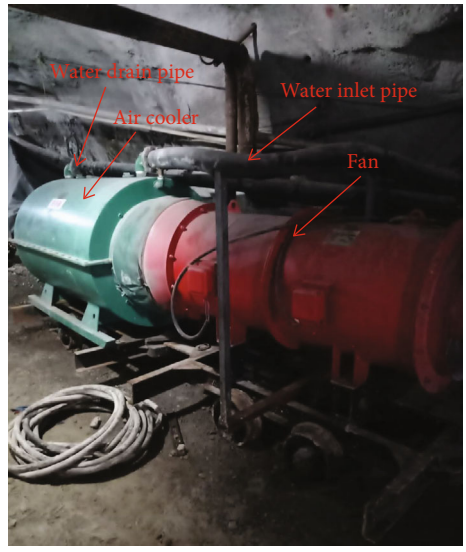

Figure 13: Equipment installation drawing.

temperature in the inlet pipe is 5.2°C, and the water temperature in the drain pipe is 13.8°C. The air handling capacity, and cooling load of the air cooler are shown in Table 4.

After the cooling system is stable, the inlet speed of the air duct is 5.8 m/s, and the air outlet temperature is 13.4°C. The on-site temperature measurement results are shown in Table 5. From the temperature comparison of each measuring point before and after cooling, the temperature is the lowest within a 1 m range of the working face and the maximum decrease is observed, 26.4°C and 8.4°C, respectively. The average temperature within 50 m of the working face is 27.2°C, with an average decrease of 7.5°C. The temperature of each measuring point can reach below 28°C. Therefore, the cooling parameters can meet the requirements of tunnel cooling.

Table 4: Cooling load of air cooler.

Air handling capacity (kg/s)	Air intake environment		Air outlet environment		Cooling load (KW)
	Temperature (°C)	Relative humidity (%)	Temperature (°C)	Relative humidity (%)	
1.5	35.1	94.2	13.4	100.0	121.1

Table 5: Temperature comparison of each measuring point before and after cooling.

Distance from working face (m)	Temperature before cooling (°C)	Temperature after cooling (°C)	Temperature difference (°C)
1	34.8	26.4	8.4
10	34.8	26.6	8.2
20	34.7	27.0	7.7
30	34.6	27.5	7.0
40	34.5	27.6	6.9
50	34.5	27.8	6.8
Average	34.7	27.2	7.5

6. Conclusions

(1) A set of cooling systems based on water source heat pump technology and employing the return air system to exhaust heat is constructed to address the issue of heat damage at the -750 m level in the Lingshan mining area. The system mainly includes refrigeration system, heat transfer system, heat removal system, and cooling system. Each system adopts closed circulation, which can effectively solve the problem of insufficient groundwater. Meanwhile, the heat removal system directly discharges heat to the return air shaft to prevent secondary heat damage during the heat removal process

(2) The heat and mass transfer model of a -750 m level, long-distance, single-headed face is constructed, and its accuracy is verified in conjunction with field practice. The distribution law of the thermal tunnel environment under various working conditions is simulated by comparing the effects of increasing inlet speed and decreasing inlet temperature. Through analysis and comparison, the optimal inlet speed and temperature range have been determined, which can reduce the temperature near the working face from 35°C to below 28°C

(3) This paper establishes a water source heat pump cooling system suitable for the Linglong Gold Mine using field practice, theoretical calculation, and numerical simulation as a reference for the application of cooling technology in metal mines under comparable conditions

Data Availability

Data can only be made available from the corresponding author.

Conflicts of Interest

There is no conflict of interest regarding the publication of this paper.

Acknowledgments

This work is financially supported by the Major Science and Technological Innovation Projects of Shandong Province (Grant No. 2019DZY05).

References

[1] H. ManChao, X. HePing, P. SuPing, and J. YaoDong, "Study on rock mechanics in deep mining engineering," *Chinese Journal of Rock Mechanics and Engineering*, vol. 24, no. 16, pp. 2803–2813, 2005.

[2] F. JianHui and W. ZongWu, *Heat and Moisture Transfer and Heat-Hazard Control*, Publishing House of Electronics Industry, Beijing, 2018.

[3] B. JjingZhi and Z. WenBin, *Theory and Practice of Comprehensive Treatment Technology for High Temperature Heat Hazard in Mines*, Emergency Mangagement Press, Beijing, 2020.

[4] L. Zhongbao, W. Jun, and Z. Shuxue, "Progress on airconditioning of coal mine," *Vacuum and Cryogenics*, vol. 8, no. 3, pp. 130–134, 2002.

[5] Q. Hua, W. Jinggang, and Z. Ziping, "Study on the ice melting and feasibility of cooling system," *Journal of China Coal Society*, vol. 25, Supplement 1, pp. 122–125, 2000.

[6] S. Xikui, L. Xuehua, and C. Weimin, "Study of cold kadiation cooling technology using ice water from mine," *Journal of Mining & Safety Engineering*, vol. 26, no. 1, pp. 105–109, 2009.

[7] D. Banks, P. L. Younger, R.-T. Arnesen, E. R. Iversen, and S. B. Banks, "Minewater chemistry: the good, the bad and the ugly," *Environmental Geology*, vol. 32, no. 3, pp. 157–174, 1997.

[8] D. Banks, H. Skarphagen, R. Wiltshire, and C. Jessop, "Mine water as a resource: space heating and cooling via use of heat pumps," *Land Contamination & Reclamation*, vol. 11, no. 2, pp. 191–198, 2003.

[9] D. Banks, A. Fraga Pumar, and I. Watson, "The operational performance of Scottish minewater-based ground source heat pump systems," *Quarterly Journal of Engineering Geology and Hydrogeology*, vol. 42, no. 3, pp. 347–357, 2009.

[10] M. H. Clarkson, D. Birks, P. L. Younger, A. Carter, and S. Cone, "Groundwater cooling at the Royal Festival Hall, London," *Quarterly Journal of Engineering Geology and Hydrogeology*, vol. 42, no. 3, pp. 335–346, 2009.

[11] D. B. Walls, D. Banks, A. J. Boyce, and N. M. Burnside, "A review of the performance of minewater heating and cooling systems," *Energies*, vol. 14, no. 19, pp. 6215–6233, 2021.

[12] G. R. Watzlaf and T. E. Ackman, "Underground mine water for heating and cooling using geothermal heat pump systems," *Mine Water and the Environment*, vol. 25, no. 1, pp. 1–14, 2006.

[13] R. Rodriguez and M. B. Diaz, "Analysis of the utilization of mine galleries as geothermal heat exchangers by means a semi-empirical prediction method," *Renewable Energy*, vol. 34, no. 7, pp. 1716–1725, 2009.

[14] A. Hall, J. A. Scott, and H. Shang, "Geothermal energy recovery from underground mines," *Renewable and Sustainable Energy Reviews*, vol. 15, no. 2, pp. 916–924, 2011.

[15] J. Raymond and R. Therrien, "Optimizing the design of a geothermal district heating and cooling system located at a flooded mine in Canada," *Hydrogeology Journal*, vol. 22, no. 1, pp. 217–231, 2014.

[16] A. P. Athresh, A. Al-Habaibeh, and K. Parker, "Innovative approach for heating of buildings using water from a flooded coal mine through an open loop based single shaft GSHP system," *Energy Procedia*, vol. 75, pp. 1221–1228, 2015.

[17] M. T. Bailey, C. J. Gandy, I. A. Watson, L. M. Wyatt, and A. P. Jarvis, "Heat recovery potential of mine water treatment systems in Great Britain," *International Journal of Coal Geology*, vol. 164, pp. 77–84, 2016.

[18] C. MeiFeng, M. MingHui, P. JiLiang, X. Xun, and G. QiFeng, "Co-mining of mineral and geothermal resources: a state-of-the-art review and future perspectives," *Chinese Journal of Engineering*, vol. 44, no. 10, p. 1681, 2022.

[19] C. MeiFeng, D. Ji, C. XiangSheng et al., "Development strategy for co-mining of the deep mineral and geothermal resources," *Strategic Study of CAE*, vol. 23, no. 6, pp. 43–51, 2021.

[20] W. ChunLong, C. Li, H. YingJie, J. MingWei, C. KeXu, and S. Kun, "Efficiency improvement and application of the groundwater heat pump cooling system in Linglong gold mine," *Geofluids*, vol. 2022, Article ID 3191735, 9 pages, 2022.

[21] H. Guojia, R. Guoqiang, and Y. Zhuang, "Research and application on preventive measure against heat disaster in Zhaolou coal mine," *Journal of China Coal Society*, vol. 36, no. 1, pp. 101–104, 2011.

[22] Y. Liang, "Theoretical analysis and practical application of coal mine cooling in Huainan mining area," *Journal of Mining & Safety Engineering*, vol. 24, no. 3, pp. 298–301, 2007.

[23] H. Manchao and X. Min, "Research and development of HEMS cooling system and heat-harm control in deep mine," *Chinese Journal of Rock Mechanics and Engineering*, vol. 27, no. 7, pp. 1353–1361, 2008.

[24] H. Manchao and G. Pingye, "Deep rock mass thermodynamic effect and temperature control measures," *Chinese Journal of Rock Mechanics and Engineering*, vol. 32, no. 12, pp. 2377–2393, 2013.

[25] H. Man-Chao, "Application of HEMS cooling technology in deep mine heat hazard control," *Mining Science and Technology*, vol. 19, no. 3, pp. 269–275, 2009.

[26] H. E. Manchao, C. A. Xiuling, X. I. Qiao et al., "Principles and technology for stepwise utilization of resources for mitigating deep mine heat hazards," *Mining Science and Technology*, vol. 20, no. 1, pp. 20–27, 2010.

[27] M. He, P. Guo, X. Chen, L. Meng, and Y. Zhu, "Research on characteris of high-temperature and control of heat-harm of Sanhejian coal mine," *Chinese Journal of Rock Mechanics and Engineering*, vol. 29, Supplement 1, pp. 2593–2597, 2010.

[28] H. Manchao and G. Pingye, "Field experimental study on heat disaster control in Xuzhou mining area," *Coal Engineering*, vol. 47, no. 4, pp. 1–4, 2015.

[29] N. XingXin, W. XiaoBin, L. XiaoChen, and L. CaiWu, "Heat treatment and ventilation optimization in a deep mine," *Advances in Civil Engineering*, vol. 2018, no. Part 6, Article ID 1529490, p. 12, 2018.

[30] G. Pingye, *Characteristics of Geothermal Field of Deep Mine and Its Heat Damage Control in China*, China University of Mining and Technology, Beijing, 2009.

[31] G. Pingye and Z. Yanyan, "Back-analysis algorithm of cooling load in deep mines," *Journal of Mining & Safety Engineering*, vol. 28, no. 3, pp. 483–487, 2011.

[32] G. Pingye, W. YanWei, D. MengMeng, P. DongYang, and L. Nan, "Research and application of methods for effectiveness evaluation of mine cooling system," *International Journal of Mining Science and Technology*, vol. 25, no. 4, pp. 649–654, 2015.

[33] Y. Shengbin, *Heat-Harm Control Technique at Great Depths with Mine Water Discharge as Cold Source in Jiahe Coal Mine*, China University of Geosciences, Beijing, 2008.

[34] M. Li, *Sink Technology of Horizontal Circulation and Operational Analysis of HEMS in Sanhejian Coal Mine*, China University of Mining and Technology, Beijing, 2010.

[35] Q. Fan, *Study of Roadway Thermal Environment and Cooling Load Analysis and Calculation*, China University of Mining and Technology, Beijing, 2015.

[36] X. Yu, L. ZiJun, L. HuaSen et al., "Modeling of the dynamic behaviors of heat transfer during the construction of roadway using moving mesh," *Case Studies in Thermal Engineering*, vol. 26, article 100958, 2021.

[37] X. Yu, L. ZiJun, C. Yin, J. MinTao, Z. MengMeng, and L. RongRong, "Synergetic mining of geothermal energy in deep mines: an innovative method for heat hazard control," *Applied Thermal Engineering*, vol. 210, article 118398, 2022.

[38] X. Yu, L. ZiJun, W. JunJian et al., "Ventilation and heat exchange characteristics in high geotemperature tunnels considering buoyancy-driven flow and groundwater flow," *International Journal of Thermal Sciences*, vol. 173, article 107400, 2022.

[39] X. Yu, L. ZiJun, T. Ming et al., "An investigation into the effect of water injection parameters on synergetic mining of geothermal energy in mines," *Journal of Cleaner Production*, vol. 382, article 135256, 2023.